



Optics Letters

Tapered suspended-core fibers for broadband supercontinuum generation and an f-2f interferometer

TRUNG LE CANH,¹ THUAN BUI DINH,¹ DUNG NGUYEN TIEN,¹ KHOA DINH XUAN,¹
NGO VINH DOAN THE,¹ HUNG LUU TIEN,¹ HIEU VAN LE,²  AND VAN THUY HOANG^{1,*} 

¹Vinh University, 182 Le Duan Street, Vinh City, Vietnam

²Faculty of Natural Sciences, Hong Duc University, 565 Quang Trung Street, Thanh Hoa City, Vietnam

*thuyhv@vinhuni.edu.vn

Received 2 January 2025; revised 6 March 2025; accepted 8 March 2025; posted 10 March 2025; published 2 April 2025

Octave-spanning supercontinuum (SC) generation typically requires high input pulse energies and long fiber lengths. Achieving such high pulse energies is feasible only with low repetition rate lasers, operating in the kHz to MHz range. In contrast, high repetition rate lasers, such as microresonator-based frequency combs (microcombs), provide lower input pulse energy. This necessitates the use of fibers with high nonlinearity, high coupling efficiency with laser sources, and tailored dispersion properties for broadband supercontinua. In this work, we present tapered fibers fabricated from lead-bismuth-gallate (PBG) glass—a material with high nonlinearity—for octave-spanning supercontinuum generation spanning from 760 to 1860 nm at low input pulse energies (0.03–0.05 nJ). The untapered sections of these fibers feature a large core diameter (10 μm) to assure high coupling efficiency with standard single-mode fibers or laser sources. At the tapered waist, the core diameter is reduced to 1.5 μm, significantly enhancing the nonlinear coefficient and enabling octave-spanning supercontinuum generation. The supercontinuum spectra align well with the optical properties of periodically poled lithium niobate (PPLN-SHG6), making these tapered fibers ideal for f-2f interferometers to measure the carrier-envelope offset frequency of microcombs. © 2025 Optica Publishing Group. All rights, including for text and data mining (TDM), Artificial Intelligence (AI) training, and similar technologies, are reserved.

<https://doi.org/10.1364/OL.554625>

Coherent octave-spanning supercontinuum (SC) generation is important for applications such as spectroscopy [1,2], biomedical imaging [3,4], and environmental sensing [5,6]. Achieving such broadband SC generation typically requires high-energy input laser pulses to enhance nonlinear effects. A high input energy also ensures a high power spectral density (PSD), which is essential for applications such as multiphoton microscopy [3] and gas or liquid detection [5,6]. However, developing nonlinear fibers that enable broadband SC generation at low input energies is also essential for compact SC light sources, where conventional laser sources with low averaged output powers can

be used as pump sources. Interestingly, these fibers are crucial in frequency combs, where they are used to broaden the initial spectral combs to the wavelength ranges required for practical applications.

Optical frequency combs, based on mode-locked lasers or microresonators, typically have narrow spectral bandwidths, often limited to just tens of nanometers [7,8]. Broadening these combs is essential to expand their application potential. However, achieving significant broadening, especially in microresonator-based frequency combs (microcombs), presents challenges due to their high repetition rate (f_{rep}). Since pulse energy is inversely proportional to f_{rep} , the high f_{rep} values of microcombs (e.g., tens of GHz) result in low individual pulse energies, which restrict spectral broadening.

This spectral broadening limitation is a significant challenge in detecting the carrier-envelope offset frequency (f_{ceo}) of microcombs using an f-2f interferometer. For successful detection, the initial spectra must be coherently broadened to an octave, covering the frequency-doubled range of periodically poled lithium niobate (PPLN) [9]. Despite advancements in microcomb technology, reliable detection of f_{ceo} remains an ongoing challenge.

Nonlinear fibers have been widely utilized as post-stage components for spectral comb broadening. In these approaches, the initial spectra are amplified using an erbium-doped fiber amplifier (EDFA) and subsequently injected into a nonlinear fiber [9–11]. Nonlinear fibers typically have small core diameters—on the order of a few micrometers—to enhance the nonlinear effects. Notwithstanding, their small cores create significant challenges in achieving high coupling efficiency with standard single-mode fibers (e.g., SMF-28) or laser sources. Furthermore, nonlinear fibers are often fabricated from silica due to its high transparency and ease of processing. However, silica's relatively low nonlinearity necessitates high-energy laser pulses for broadband SC generation, limiting its compatibility with f-2f interferometers.

In this Letter, we develop tapered suspended-core fibers fabricated from lead-bismuth-gallate (PBG) glass, a material with high nonlinearity. These fibers feature a large core in the untapered section, ensuring high coupling efficiency with standard

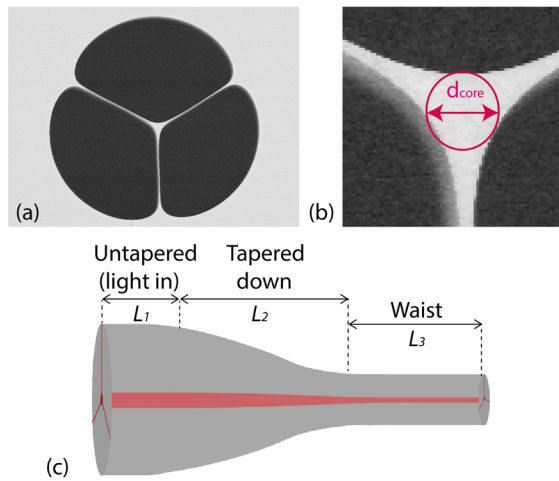


Fig. 1. (a) Image of the suspended-core fibers. The fibers have three air-holes at the cladding; (b) zoom-in of the center section; (c) schemes of tapered fibers. The length of the untapered section is $L_1 = 1$ cm, the tapered-down $L_2 = 3$ cm, and the waist $L_3 = 2$ cm.

single-mode fibers or laser sources. The tapered waist region, with its small core diameter, enables octave-spanning SC generation using low-energy laser pulses, making it compatible with f-2f interferometers to detect f_{ceo} of microcombs. This work includes numerical calculations of the linear properties, such as dispersion, for tapered fibers with varying core diameters. Next, we perform numerical simulations of SC generation using femtosecond laser pulses at 1550 nm.

We develop suspended-core fibers for SC generation due to their high nonlinearity, which arises from their small core size [12,13]. These fibers feature a core surrounded by cladding air-holes (see Figs. 1(a) and 1(b)). The combination of a small core and the high refractive index contrast between the core and cladding ensures strong light confinement, resulting in enhanced nonlinearity for spectral broadening.

Conventional suspended-core fibers with small core diameters have low coupling efficiency with standard single-mode fibers. To address this limitation, we propose the use of tapered suspended-core fibers. In this design, the untapered section, with a core diameter (d_{core}) of 10 μm , enables a high coupling efficiency. The tapered waist section, with a reduced core diameter ($d_{core} \approx 1.5$ μm), achieves a high nonlinear coefficient, facilitating broadband SC generation (see Fig. 1(c)).

It is worth noting that various materials have recently been utilized for nonlinear fibers, including gases, liquids, silica, ZBLAN, and chalcogenide glasses [14]. Gases and liquid-filled fibers require complex experimental setups involving gas or liquid cells, making them unsuitable for compact systems [15,16]. Silica and ZBLAN glasses, on the other hand, exhibit relatively low nonlinear refractive indices. Chalcogenide glasses offer high nonlinearity and transparency, but are only compatible with SC generation in the mid-infrared range [14].

In this work, the fibers are made from PBG glass with high transparency and high nonlinearity [17]. The nonlinear refractive index is $n_2 = 4.3 \times 10^{-19}$ m^2/W [17]. This value is 16 times greater than the nonlinear refractive index of silica, enabling significantly enhanced nonlinear effects. The combination of the glass's high nonlinearity, high coupling efficiency, and the small core size of the waist region facilitates an octave-spanning SC generation with low input pulse energy (e.g., 0.05 nJ).

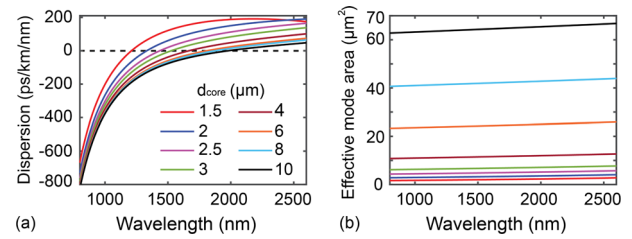


Fig. 2. (a) Dispersion and (b) effective mode area of suspended-core fibers with various core diameters.

Additionally, PBG glass demonstrates robust mechanical strength and exceptional thermo-mechanical stability, making it an ideal material for fiber fabrication using the conventional stack-and-draw method. This glass has been successfully utilized to fabricate nonlinear photonic crystal fibers (PCFs) with sophisticated structures designed for SC generation [18,19]. Its advantageous properties also enable the fabrication of suspended-core fibers with large core diameters (up to 10 μm) via the stack-and-draw technique. The tapering process can be performed using either the conventional “heating-and-stretching” method or a fiber drawing tower, as detailed in [20].

A tapered fiber typically consists of five sections: the untapered (light-in), tapered-down, waist, tapered-up, and untapered (light-out) [20]. To taper a fiber with a core diameter of $d_{core} = 10$ μm down to $d_{core} = 1.5$ μm , the tapered-down section typically has a length of 2–3 cm, while the waist length ranges from 22 to 53 cm [20]. As discussed in the previous work [21], and also in the following sections, spectral broadening predominantly occurs over a short propagation length (e.g., 5 cm) within the waist section. Therefore, in this work, we consider the nonlinear propagation only in the untapered (light-in) part with length $L_1 = 1$ cm, the tapered-down with $L_2 = 3$ cm, and the waist with $L_3 = 2$ cm. The tapered-up and untapered (light-out) sections are excluded from the analysis, as they do not significantly contribute to spectral broadening [21].

The tapering process reduces the effective mode area (A_{eff}), thereby enhancing the nonlinear coefficient. In the untapered section with $d_{core} = 10$ μm , the effective mode area ranges from 62 to 67 μm^2 over the wavelength range of 800–2600 nm (see Fig. 2(b)). The mode properties (i.e., polarization and mode area) at the untapered section are compatible with a single-mode fiber, and we numerically calculate the coupling efficiency between these fibers being 85%. As the fiber transitions through the tapered-down section, the effective mode area decreases further. In the waist section with $d_{core} = 1.5$ μm , the effective mode area is reduced to 1.6–2.7 μm^2 (Fig. 2(b)).

Additionally, the tapering process significantly modifies the dispersion, which is critical for broadband SC generation. Specifically, the dispersion shifts toward the anomalous dispersion regime, and the zero-dispersion wavelength (ZDW) moves to shorter wavelengths, as shown in Fig. 2(a). This blueshifting of the ZDW enables blueshifted dispersive waves. Consequently, the dispersive waves align with the frequency-doubled photons of PPLN for f-2f interferometers, as shown in Fig. 3.

The evolution of input pulses in the tapered fibers is numerically studied by solving the nonlinear Schrödinger equation

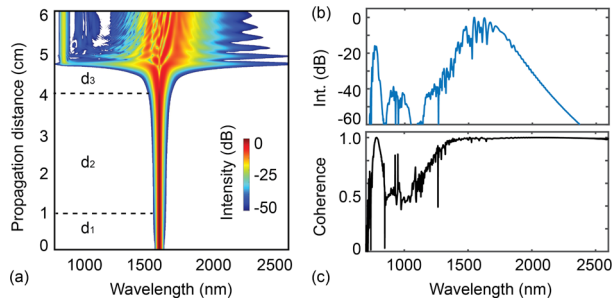


Fig. 3. (a) Evolution of a laser pulse in the tapered fiber; (b) output SC spectrum and (c) coherence. The input pulse energy is 0.05 nJ, the pulse duration is 200 fs, and the pump wavelength is 1550 nm.

(NLSE) by the split-step method [22], as given in Eq. (1):

$$\frac{\partial A}{\partial z} = -\frac{\alpha}{2}A + \sum_{k \geq 2} \frac{i^{k+1}}{k!} \beta_k \frac{\partial^k A}{\partial T^k} + i\gamma \left(1 + i\tau_{shock} \frac{\partial}{\partial T} \right) \times \left\{ (1 - f_R) |A|^2 + f_R \int h(T - T') |A(T - T')|^2 dT' \right\} A, \quad (1)$$

where A is the envelope function, $\tau_{shock} = \frac{1}{\omega_0}$ is the shock wave, $f_R = 0.05$ is the Raman fraction, $h(T)$ is the response Raman function [17], and $\gamma = \frac{2\pi n_2}{\lambda A_{eff}}$ is the nonlinear coefficient. For tapered fibers, the nonlinear coefficient (γ), loss (α), and dispersion (β_k) are functions of propagation length (z) in NLSE [21].

Fiber losses consist of material attenuation and confinement loss. In this work, the confinement loss is negligible due to the high refractive index contrast between the core and the cladding. The fiber loss is assumed to remain constant across the wavelength range, with a value of 16 dB/m [18,19]. Note that a short fiber sample (6 cm) is used for SC generation; consequently, the fiber loss does not significantly limit the spectral broadening.

Simulation of SC generation in the tapered suspended-core fiber is shown in Fig. 3. The input pulse energy is 0.05 nJ, the pulse duration is 200 fs, and the pump wavelength is 1550 nm.

The input pulses do not experience significant spectral broadening in the untapered and tapered-down sections because of the large core diameters. An octave-spanning spectrum (from 760 to 1860 nm) is generated in the waist section after a short length of propagation (1 cm from the offset point of the waist).

The SC generation is induced by soliton fission, occurring approximately at 5 cm of the propagation—at 1 cm in the waist (see Fig. 3(a)). The output spectrum is not flat, as most of the power spectral density is distributed around the pump wavelengths, spanning from 1450 to 1850 nm. Dispersive waves are created around 760 nm, reaching an intensity level of approximately -15 dB (see Fig. 3(b)).

Interestingly, the SC spectrum matches very well with the properties of PPLN (SHG6), which has frequency-doubled photons from 783 to 826 nm [23]. Therefore, although the SC generation in the tapered fiber is not flat, the spectral properties make it well-suited for effective use in an f-2f interferometer.

We consider the coherence $g_{12}^1(\lambda)$ (i.e., pulse-to-pulse stability) of SC generation under the influence of vacuum noise and laser noise [22,24].

Laser noise refers to random fluctuations in the amplitude and pulse duration of individual pulses relative to their average

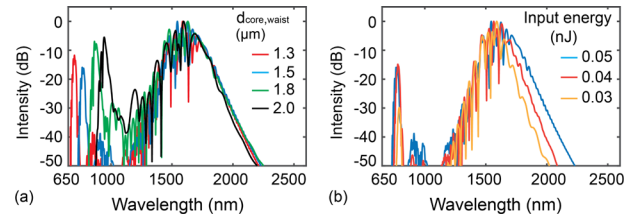


Fig. 4. (a) SC generation in the tapered fibers with 0.05 nJ input pulse energy. The fibers have various core diameters of the waist part; (b) SC generation in the tapered fiber with $d_{core} = 1.5 \mu\text{m}$ and various input pulse energies. The duration of input laser pulses is 200 fs, and the pump wavelength is 1550 nm.

values [24]. In this study, the root mean square (RMS) amplitude fluctuation is 1%.

Despite being induced by soliton dynamics in the anomalous dispersion regime, SC generation exhibits high coherence, as shown in Fig. 3(c). Both the dispersive waves and the spectral region near the pump wavelengths maintain coherence values close to 1. This high coherence is attributed to a low input energy. In this case, modulation instability requires longer propagation distances to amplify input noises significantly [22].

The high coherence, corresponding to the high pulse-to-pulse stability of the SC spectra, is crucial for applications in octave-spanning frequency combs and detection of f_{ceo} .

The material dispersion of glass, described by the Sellmeier equation [18], causes discrepancies in the dispersion between simulated and experimental results, especially in small core fibers and at long wavelengths ($\lambda > 2 \mu\text{m}$). However, these dispersion differences are minor and have a slight impact on SC generation [19]. Errors during fiber fabrication can lead to slight discrepancies between the actual geometrical structure of a fabricated fiber and the proposed design, resulting in modifying the properties of SC generation. Since spectral broadening predominantly occurs in the waist section, altering its core diameter significantly influences SC generation. For example, as the core diameter of the waist increases from 1.3 to 2 μm , the dispersive wave shifts toward longer wavelengths, from 700 to 940 nm (see Fig. 4(a)). Although such deviations in the core diameter can lead to dispersive wave shifting, these fibers still achieve octave-spanning SC generation and remain compatible with the properties of PPLN (SHG6) used for an f-2f interferometer.

A pulse energy of 0.05 nJ was used to generate SC in the tapered fiber, as shown in Figs. 3 and 4(a). The fiber's high nonlinearity enables broad SC generation even with lower input pulse energies. To investigate this further, SC generation is studied with pulse energies of 0.04 and 0.03 nJ, as illustrated in Fig. 4(b). Reducing the pulse energy from 0.05 to 0.03 nJ does not significantly shift the position of the dispersive waves, which remain near 760 nm. However, the intensity of the dispersive waves decreases noticeably, with a 0.03 nJ pulse energy resulting in intensities 30 dB lower than those near the pump wavelength (Fig. 4(b)).

Microcombs typically operate with high f_{rep} , in the tens of gigahertz range, resulting in low energy per pulse. For example, microcombs with $f_{rep} = 20$ GHz and an average power of 2 W (after amplification with an EDFA) are used to make an octave-spanning SC generation. In this case, the pulse energy is 0.1 nJ. Assuming a coupling efficiency of approximately 50% between the comb source and the tapered fiber, a pulse energy of 0.05 nJ is injected into the fiber for spectral broadening.

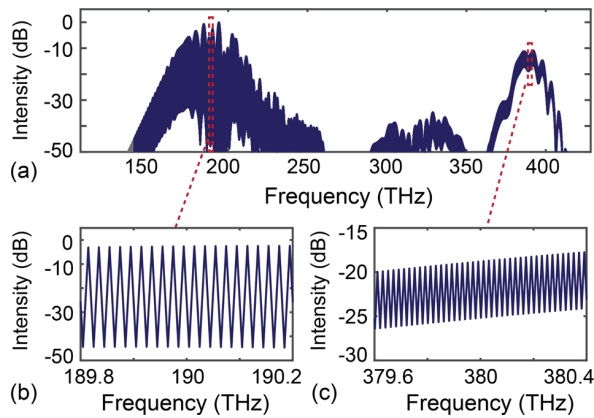


Fig. 5. Tapered fiber is used to broaden microcombs with $f_{rep} = 20$ GHz. (a) Octave-spanning frequency combs are achieved via input pulses with an energy of 0.05 nJ and a duration of 200 fs; (b)–(c) zoom-in of the spectrum at 190 THz ($\lambda = 1577.85$ nm) and at 380 THz ($\lambda = 788.9$ nm).

This setup achieves an octave-spanning frequency comb spectrum, encompassing frequency-doubled photons generated in a PPLN (SHG6) [23] (see Figs. 5(a)–5(c)). In an f - $2f$ interferometer, the spectral components around 380 THz ($\lambda = 788.9$ nm) have frequencies given by $f_1 = f_{ceo} + nf_{rep}$, while those at 190 THz ($\lambda = 1577.85$ nm) have frequencies $f_2 = f_{ceo} + mf_{rep}$. When the f_2 component is frequency-doubled, it becomes $2f_2 = 2f_{ceo} + 2mf_{rep}$. If both signals (i.e., f_1 and $2f_2$) are detected by a fast photodiode, the RF beat-note frequencies are given by $\Delta f = f_{ceo} + |2m - n|f_{rep}$ [9]. It is important to note that f_{ceo} is determined by the initial frequency combs and does not depend on the spectral broadening process of SC generation in the fiber. Figure 5 presents an SC spectrum with initial microcombs, and we do not plot a value of f_{ceo} detected by a photodiode.

In this work, the input pulse energy, ranging from 0.03 to 0.05 nJ, is significantly lower than the energy requirements of commercial packaged supercontinuum generation waveguides and comb offset stabilization modules (COSMO) [25]. In comparison, commercial COSMO systems typically require input energies between 0.2 and 1 nJ, along with pulse durations of approximately 250 fs, to enable detecting f_{ceo} of frequency combs.

The large core of the untapered section allows the fibers to achieve high coupling efficiency with high-power laser sources without fiber damage. Moreover, the high transparency of the PBG glass enables SC generation up to the mid-IR range. With input pulses of 100 fs duration and 2 nJ energy, the tapered fiber (with waist $d_{core} = 2.0$ μm) provides SC generation spanning two octaves from 580 to 3000 nm. This broad SC spectrum in the mid-IR range has potential applications in mid-infrared spectroscopy and optical coherence tomography (OCT).

In conclusion, the tapered fibers, characterized by a small core at the waist to enhance nonlinearity, have been explored for coherent octave-spanning SC generation with low input pulse energy. The large core at the untapered section ensures high coupling efficiency with standard single-mode fibers or laser sources. This design enables tapered fibers to operate effectively with commercial compact femtosecond laser sources, facilitating broadband SC generation. Moreover, despite using low input pulse energy, the high nonlinearity of the tapered fibers allows for the generation of an octave-spanning SC spectrum in

a short fiber length (6 cm). These properties make tapered fibers well-suited for compact SC sources.

One significant application of tapered fibers is in f - $2f$ interferometers for detecting f_{ceo} of frequency combs, particularly microcombs. In comparison, the commercial COSMO device requires input pulse energy of at least 0.2 nJ and a pulse duration of 250 fs to function effectively [25]. Achieving such pulse energy is challenging for microcombs due to their high repetition rates. However, the tapered fibers can operate with input pulse energy as low as 0.05 nJ—four times lower—greatly simplifying the detection of f_{ceo} of frequency combs. This advancement paves the way for broader applications of microcombs in precision metrology, such as high-resolution mid-infrared molecular spectroscopy [26] and optically steered time scales [27].

Funding. Vietnam's Ministry of Education and Training (B2024-TDV-07).

Disclosures. The authors declare no conflicts of interest.

Data availability. Data underlying the results presented in this Letter are not publicly available but may be obtained from the authors upon reasonable request.

REFERENCES

- S. A. Diddams, L. Hollberg, and V. Mbele, *Nature* **445**, 627 (2007).
- N. Picqué and T. Hänsch, *Nat. Photonics* **13**, 146 (2019).
- C. Poudel and C. F. Kaminski, *J. Opt. Soc. Am. B* **36**, A139 (2019).
- V. T. Hoang, Y. Boussafa, L. Sader, *et al.*, *Front. Photon.* **3**, 940902 (2022).
- K. E. Jahromi, M. Nematollahi, R. Krebbers, *et al.*, *Opt. Express* **29**, 12381 (2021).
- T. Mikkonen, T. Hieta, G. Genty, *et al.*, *Phys. Chem. Chem. Phys.* **24**, 19481 (2022).
- T. J. Kippenberg, R. Holzwarth, and S. A. Diddams, *Science* **332**, 555 (2011).
- A. Pasquazi, M. Peccianti, L. Razzari, *et al.*, *Phys. Rep.* **729**, 1 (2018).
- P. Del'Haye, A. Coillet, T. Fortier, *et al.*, *Nat. Photonics* **10**, 516 (2016).
- E. S. Lamb, D. R. Carlson, D. D. Hickstein, *et al.*, *Phys. Rev. Appl.* **9**, 024030 (2018).
- N. Hoghooghi, S. Xing, P. Chang, *et al.*, *Light: Sci. Appl.* **11**, 264 (2022).
- A. Hartung, A. M. Heidt, and H. Bartelt, *Opt. Express* **19**, 12275 (2011).
- T. L. Canh, V. T. Hoang, H. L. Van, *et al.*, *Opt. Mater. Express* **10**, 1733 (2020).
- T. Sylvestre, E. Genier, A. N. Ghosh, *et al.*, *J. Opt. Soc. Am. B* **38**, F90 (2021).
- F. Belli, A. Abdolvand, W. Chang, *et al.*, *Optica* **2**, 292 (2015).
- V. T. Hoang, R. Kasztelanovic, A. Filipkowski, *et al.*, *Opt. Mater. Express* **9**, 2264 (2019).
- J. Cimek, N. Liaros, S. Couris, *et al.*, *Opt. Mater. Express* **7**, 3471 (2017).
- G. Stepniewski, J. Pniewski, D. Pysz, *et al.*, *Sensors* **18**, 4127 (2018).
- H. V. Le, V. T. Hoang, G. Stepniewski, *et al.*, *Opt. Express* **29**, 39586 (2021).
- A. N. Ghosh, M. Meneghetti, C. R. Petersen, *et al.*, *J. Phys. Photonics* **1**, 044003 (2019).
- L. C. Van, N. V. T. Minh, B. T. Le Tran, *et al.*, *Opt. Commun.* **537**, 129441 (2023).
- J. M. Dudley, G. Genty, and S. Coen, *Rev. Mod. Phys.* **78**, 1135 (2006).
- Thorlabs-Inc., "Periodically poled lithium niobate," <https://www.thorlabs.com/catalogpages/693.pdf>.
- E. Genier, P. Bowen, T. Sylvestre, *et al.*, *J. Opt. Soc. Am. B* **36**, A161 (2019).
- Octave-Photonics, "Products and services," <https://www.octavephotonics.com/products>.
- D. B. A. Tran, O. Lopez, M. Manceau, *et al.*, *APL Photonics* **9**, 030801 (2024).
- H. Hachisu, F. Nakagawa, Y. Hanado, *et al.*, *Sci. Rep.* **8**, 4243 (2018).